Applied Mathematical Modelling 36 (2012) 1766–1775

Contents lists available at SciVerse ScienceDirect

Applied Mathematical Modelling

journal homepage: www.elsevier.com/locate/apm

On a finite crack partially penetrating two circular inhomogeneities and some related problems

X. Wang [a,*], E. Pan [b,c]

[a] School of Mechanical and Power Engineering, East China University of Science and Technology, Shanghai 200237, PR China
[b] Dept. of Civil Engineering, University of Akron, Akron, OH 44325-3905, USA
[c] Dept. of Applied Mathematics, University of Akron, Akron, OH 44325-3905, USA

ARTICLE INFO

Article history:
Received 30 June 2008
Received in revised form 26 August 2011
Accepted 1 September 2011
Available online 12 September 2011

Keywords:
Crack
Stress intensity factor
Two circular inhomogeneities
Apollonius circle
Closed-form solutions

ABSTRACT

We investigate a Mode-III finite slit crack partially penetrating two circular inhomogeneities embedded in an unbounded matrix. In order to obtain analytical solutions, it is assumed that the two circular inhomogeneity–matrix interfaces are Apollonius circles with respect to the two crack tips (or equivalently the two crack tips are just mutually image points with respect to each one of the two circular interfaces). Particularly closed-form expressions of the stress intensity factors at the two crack tips are obtained even though only series form solutions to the original boundary value problem can be derived. The loadings considered in this research include: (i) remote uniform anti-plane shearing; (ii) a straight screw dislocation at any position of the three-phase composite system; (iii) a Zener-Stroh crack. The results are verified by comparison with existing solutions. The related problem of a circular hole partially merged in two circular inhomogeneities is also addressed, with closed-form expressions of the stress concentration factors derived.

1. Introduction

Crack problems in fibrous composites are an important research topic. In previous studies only crack problems for an isolated fiber (or inhomogeneity) were considered [1–4]. As a result the interaction effects among neighboring fibers on the propagation of cracks were not taken into account in previous modeling attempts. For a better understanding of the failure mechanism in fibrous composites the crack problems for multiple fibers should be addressed. Apparently it is extremely challenging to analytically address the crack problems for multiple fibers.

In this study we consider the problem of a Mode-III finite crack with its two tips lodged in two circular elastic inhomogeneities embedded in an unbounded matrix. To analytically investigate this problem, we assume that the two circular inhomogeneity–matrix interfaces are Apollonius circles with respect to the two crack tips (or equivalently the two crack tips are just mutually image points with respect to each one of the two circular interfaces). The problem investigated here can be considered as an extension of our recent study [4] on a finite crack penetrating a single circular inhomogeneity, and can also be considered as an extension of the study by Honein et al. [5] on two circular inhomogeneities in the absence of any crack. The most exciting finding of this research is that closed-form expressions of the Mode-III stress intensity factors (SIFs) at the two crack tips, which are the most important parameters in fracture mechanics [6], can be obtained for any kind of loading conditions even though only series form solutions can be derived for the original boundary value problem. The related problem of a circular hole partially merged in two circular inhomogeneities is also addressed. Here the circular hole intersects the

* Corresponding author.
E-mail address: xuwang_sun@hotmail.com (X. Wang).

0307-904X/$ - see front matter
doi:10.1016/j.apm.2011.09.014

two circular inhomogeneities at a common vertex angle $\pi/2$, which is an extension of the 2D *snowman* type of an object studied by Palaniappan [7]. Interestingly closed-form expressions of the stress concentration factors (SCFs) can be derived.

2. Basic equations

We consider two circular inhomogeneities embedded in an unbounded matrix, as shown in Fig. 1. The two inhomogeneities and the matrix are linearly elastic with the associated shear moduli μ_1 for the right inhomogeneity of radius $(x_1-x_2)/2$, μ_2 for the matrix, and μ_3 for the left inhomogeneity of unit radius. The left circular interface between the left inhomogeneity and the surrounding matrix and the right circular interface between the right inhomogeneity and the surrounding matrix are perfect: both the traction and the displacement are *continuous* across the two interfaces. The Cartesian coordinate system is established in such a way that the x-axis passes through the centers of the two inhomogeneities, and the origin is at the center of the left inhomogeneity. The right circular interface intersects the x-axis at $(x_2,0)$ and $(x_1,0)$, $(x_1>x_2>1)$. In addition there exists a Mode-III finite slit crack on the x-axis with its left crack tip at $(1/a,0)$ $\left(a=\frac{1+x_1x_2+\sqrt{(x_1^2-1)(x_2^2-1)}}{x_1+x_2}, x_2<a<x_1\right)$ within the left inhomogeneity and with its right crack tip at $(a,0)$ within the right inhomogeneity. Apparently the two crack tips are mutually image points with respect to each one of the two circular interfaces. Equivalently the two circular inhomogeneity–matrix interfaces are Apollonius circles [7] with respect to the two crack tips, i.e., $\frac{|z-a|}{|z-1/a|}=a$ when $|z|=1$; and $\frac{|z-a|}{|z-1/a|}=aR$, $\left(R=\frac{1-x_1x_2+\sqrt{(x_1^2-1)(x_2^2-1)}}{x_2-x_1}\right)$ when $|z-(x_1+x_2)/2|=(x_1-x_2)/2$. Here the complex variable z is defined as $z=x+iy$.

The loadings considered in this research include: (i) remote uniform anti-plane shearing σ_{zy}^{∞}; (ii) a straight screw dislocation with Burgers vector b located at any position of the three-phase composite system; (iii) a Zener-Stroh crack with a total Burgers vector b. In the following discussions the subscripts 1, 2 and 3 are adopted to identify the quantities in the right inhomogeneity, the surrounding unbounded matrix and the left inhomogeneity.

We first introduce the following Möbius transform [8]

$$z=\frac{\xi-a}{a\xi-1}, \tag{1}$$

which maps respectively the right and left circular interfaces in the z-plane onto two concentric circles $|\xi|=R$ and $|\xi|=1$ in the ξ-plane ($\xi=u+iv$) as shown in Fig. 2. The right crack tip $z=a$ is mapped to $\xi=0$, whilst the left crack tip $z=1/a$ is mapped to $\xi=\infty$. Now the crack of finite length is mapped to the semi-infinite negative u-axis in the ξ-plane. In addition $z=\infty$ is mapped to $\xi=1/a$.

We further consider the following conformal mapping function

$$\xi=\zeta^2, \tag{2}$$

which maps the cracked ξ-plane onto the right ζ-plane ($\zeta=\delta+i\eta$), with the semi-infinite negative u-axis in the ξ-plane being mapped to the straight boundary $\delta=0$ in the ζ-plane as shown in Fig. 3. The two concentric circles $|\zeta|=R$ and $|\zeta|=1$ in the ξ-plane are mapped to two concentric half-circles $|\zeta|=\sqrt{R}$, $\delta\geqslant0$ and $|\zeta|=1$, $\delta\geqslant0$ in the ζ-plane. We now have three boundaries to address in the ζ-plane: one straight boundary $\delta=0$ and two half-circular interfaces $|\zeta|=\sqrt{R}$, $\delta\geqslant0$ and $|\zeta|=1$, $\delta\geqslant0$.

In view of Eqs. (1) and (2), we have

$$z=m(\zeta)=\frac{\zeta^2-a}{a\zeta^2-1}, \tag{3}$$

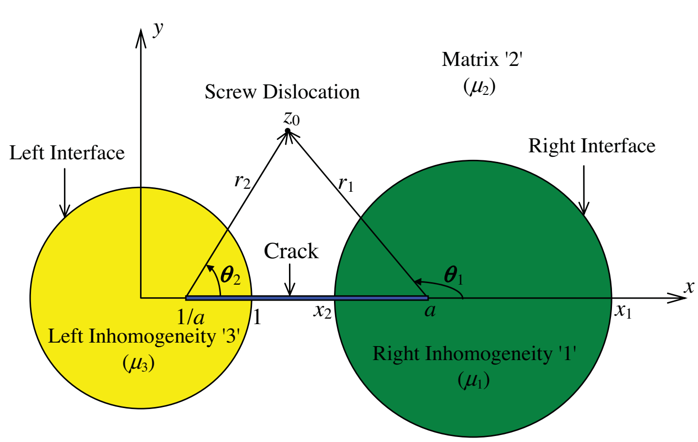

Fig. 1. A crack partially penetrating two circular inhomogeneities in the original z-plane.

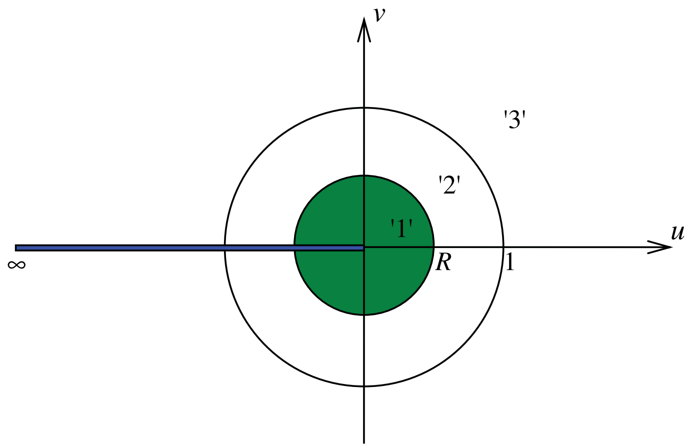

Fig. 2. The mapped ξ-plane.

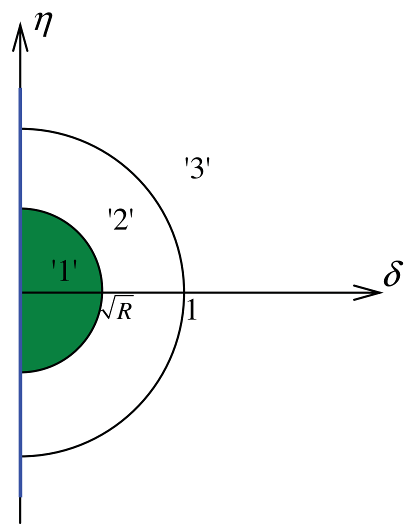

Fig. 3. The mapped ζ-plane.

or inversely

$$\zeta = m^{-1}(z) = \sqrt{\frac{z-a}{az-1}}. \tag{4}$$

The anti-plane displacement w and stresses can be expressed in terms of one analytic function $f(\zeta) = f(m(\zeta)) = f(z)$ as [9]

$$\begin{aligned} &w = Im\{f(\zeta)\}, \\ &\sigma_{zy} + \mathrm{i}\sigma_{zx} = \mu \tfrac{f'(\zeta)}{m'(\zeta)}. \end{aligned} \tag{5}$$

3. Remote uniform anti-plane shearing σ_{zy}^{∞}

In this remote uniform loading case we observe that the singular behavior $f_{2s}(\zeta)$ of $f_2(\zeta)$ defined in the matrix is

$$f_{2s}(\zeta) = \frac{\sigma_{zy}^{\infty}(1-a^2)}{2\mu_2 a}\frac{1}{\sqrt{a}\zeta - 1}, \tag{6}$$

which indicates that $f_2(\zeta)$ has a first-order pole at $\zeta = 1/\sqrt{a}$. We can satisfy the traction-free condition $Re\{f(\zeta)\} = 0$ on the straight boundary $\delta = 0$ by adding another *imaginary* pole of the same magnitude at $\zeta = -1/\sqrt{a}$. Consequently we now have only two *intact* circular interfaces $|\zeta| = \sqrt{R}$ and $|\zeta| = 1$ to address. The singular behavior $f_0(\zeta)$ of $f_2(\zeta), (\sqrt{R} < |\zeta| < 1)$ is now changed to

$$f_0(\zeta) = \frac{\sigma_{zy}^{\infty}(1-a^2)}{2\mu_2 a}\left(\frac{1}{\sqrt{a}\zeta - 1} + \frac{1}{\sqrt{a}\zeta + 1}\right). \tag{7}$$

In the following we will derive the three analytic functions $f_i(\zeta)$, $(i=1-3)$ which characterize the elastic field of the cracked three-phase composite system. The continuity conditions of traction and displacement across the two interfaces $|\zeta|=\sqrt{R}$ and $|\zeta|=1$ can be expressed in terms of $f_1(\zeta)$ defined in the right inhomogeneity, $f_2(\zeta)$ defined in the matrix and $f_3(\zeta)$ defined in the left inhomogeneity as

$$\begin{aligned} &f_1^+(\zeta)-\bar{f}_1^-\left(\tfrac{R}{\zeta}\right)=f_2^-(\zeta)-\bar{f}_2^+\left(\tfrac{R}{\zeta}\right),\\ &\mu_1\left[f_1^+(\zeta)+\bar{f}_1^-\left(\tfrac{R}{\zeta}\right)\right]=\mu_2\left[f_2^-(\zeta)+\bar{f}_2^+\left(\tfrac{R}{\zeta}\right)\right], \end{aligned}\quad (|\zeta|=\sqrt{R}) \tag{8}$$

and

$$\begin{aligned} &f_2^+(\zeta)-\bar{f}_2^-\left(\tfrac{1}{\zeta}\right)=f_3^-(\zeta)-\bar{f}_3^+\left(\tfrac{1}{\zeta}\right),\\ &\mu_2\left[f_2^+(\zeta)+\bar{f}_2^-\left(\tfrac{1}{\zeta}\right)\right]=\mu_3\left[f_3^-(\zeta)+\bar{f}_3^+\left(\tfrac{1}{\zeta}\right)\right], \end{aligned}\quad (|\zeta|=1) \tag{9}$$

where the superscripts "+" and "−" denote the limit values from the inner and outer sides of the circles $|\zeta|=\sqrt{R}$ and $|\zeta|=1$.

It follows from Eq. (8)$_1$ that

$$\begin{aligned} f_2(\zeta)&=-\bar{f}_1\left(\tfrac{R}{\zeta}\right)+\sum_{n=1}^{+\infty}A_n(\zeta^{2n-1}+R^{2n-1}\zeta^{-(2n-1)})+f_0(\zeta)+\bar{f}_0\left(\tfrac{R}{\zeta}\right),\\ \bar{f}_2\left(\tfrac{R}{\zeta}\right)&=-f_1(\zeta)+\sum_{n=1}^{+\infty}A_n(\zeta^{2n-1}+R^{2n-1}\zeta^{-(2n-1)})+f_0(\zeta)+\bar{f}_0\left(\tfrac{R}{\zeta}\right), \end{aligned} \tag{10}$$

where A_n ($n=1,2,\ldots,+\infty$) are *real* constants to be determined.

Substitution of Eq. (10) into Eq. (8)$_2$ yields

$$f_1^+(\zeta)+\bar{f}_1^-\left(\frac{R}{\zeta}\right)=\Gamma_1\left[\sum_{n=1}^{+\infty}A_n(\zeta^{2n-1}+R^{2n-1}\zeta^{-(2n-1)})+f_0(\zeta)+\bar{f}_0\left(\frac{R}{\zeta}\right)\right],\quad (|\zeta|=\sqrt{R}) \tag{11}$$

where $\Gamma_1=\frac{2\mu_2}{\mu_1+\mu_2}$, $(0\leqslant\Gamma_1\leqslant 2)$.

By applying the Liouville's theorem, we obtain

$$\begin{aligned} f_1(\zeta)&=\Gamma_1\left[\sum_{n=1}^{+\infty}A_n\zeta^{2n-1}+f_0(\zeta)\right],\\ \bar{f}_1\left(\tfrac{R}{\zeta}\right)&=\Gamma_1\left[\sum_{n=1}^{+\infty}A_nR^{2n-1}\zeta^{-(2n-1)}+\bar{f}_0\left(\tfrac{R}{\zeta}\right)\right]. \end{aligned} \tag{12}$$

Consequently it follows from Eqs. (10) and (12) that

$$f_2(\zeta)=\sum_{n=1}^{+\infty}A_n[\zeta^{2n-1}+(1-\Gamma_1)R^{2n-1}\zeta^{-(2n-1)}]+f_0(\zeta)+(1-\Gamma_1)\bar{f}_0\left(\frac{R}{\zeta}\right).\quad (\sqrt{R}<|\zeta|<1). \tag{13}$$

Similarly it follows from Eq. (9)$_1$ that

$$\begin{aligned} f_2(\zeta)&=-\bar{f}_3\left(\tfrac{1}{\zeta}\right)+\sum_{n=1}^{+\infty}B_n(\zeta^{2n-1}+\zeta^{-(2n-1)})+f_0(\zeta)+\bar{f}_0\left(\tfrac{1}{\zeta}\right),\\ \bar{f}_2\left(\tfrac{1}{\zeta}\right)&=-f_3(\zeta)+\sum_{n=1}^{+\infty}B_n(\zeta^{2n-1}+\zeta^{-(2n-1)})+f_0(\zeta)+\bar{f}_0\left(\tfrac{1}{\zeta}\right), \end{aligned} \tag{14}$$

where B_n ($n=1,2,\ldots,+\infty$) are also *real* constants to be determined.

Substitution of Eq. (14) into Eq. (9)$_2$ yields

$$f_3^-(\zeta)+\bar{f}_3^+\left(\frac{1}{\zeta}\right)=\Gamma_2\left[\sum_{n=1}^{+\infty}B_n(\zeta^{2n-1}+\zeta^{-(2n-1)})+f_0(\zeta)+\bar{f}_0\left(\frac{1}{\zeta}\right)\right],\quad (|\zeta|=1), \tag{15}$$

where $\Gamma_2=\frac{2\mu_2}{\mu_3+\mu_2}$, $(0\leqslant\Gamma_2\leqslant 2)$.

By applying the Liouville's theorem, we obtain

$$\begin{aligned} f_3(\zeta)&=\Gamma_2\left[\sum_{n=1}^{+\infty}B_n\zeta^{-(2n-1)}+f_0(\zeta)\right],\\ \bar{f}_3\left(\tfrac{1}{\zeta}\right)&=\Gamma_2\left[\sum_{n=1}^{+\infty}B_n\zeta^{2n-1}+\bar{f}_0\left(\tfrac{1}{\zeta}\right)\right]. \end{aligned} \tag{16}$$

Consequently it follows from Eqs. (14) and (16) that

$$f_2(\zeta) = \sum_{n=1}^{+\infty} B_n[(1-\Gamma_2)\zeta^{2n-1} + \zeta^{-(2n-1)}] + f_0(\zeta) + (1-\Gamma_2)\bar{f}_0\left(\frac{1}{\zeta}\right).(\sqrt{R} < |\zeta| < 1) \tag{17}$$

Up to now we have obtained two expressions (13) and (17) of $f_2(\zeta)$. The compatibility condition of $f_2(\zeta)$ will result in the following set of linear algebraic equations

$$\begin{aligned} &A_n + (\Gamma_2 - 1)B_n = (\Gamma_2 - 1)\tfrac{\sigma_{zy}^{\infty}(a^2-1)a^{-(2n+1)/2}}{\mu_2}, \\ &(\Gamma_1 - 1)A_n + R^{-(2n-1)}B_n = (1-\Gamma_1)\tfrac{\sigma_{zy}^{\infty}(a^2-1)a^{(2n-3)/2}}{\mu_2}, \end{aligned} \quad (n = 1, 2, \ldots, +\infty) \tag{18}$$

through which the real unknowns A_n and B_n can be uniquely determined as

$$\begin{aligned} A_n &= \tfrac{\sigma_{zy}^{\infty}(a^2-1)}{\mu_2}\tfrac{(\Gamma_2-1)\left[a^{-(2n+1)/2}+(\Gamma_1-1)a^{(2n-3)/2}R^{(2n-1)}\right]}{1-R^{(2n-1)}(\Gamma_1-1)(\Gamma_2-1)}, \\ B_n &= \tfrac{\sigma_{zy}^{\infty}(a^2-1)}{\mu_2}\tfrac{(1-\Gamma_1)R^{(2n-1)}\left[a^{(2n-3)/2}+(\Gamma_2-1)a^{-(2n+1)/2}\right]}{1-R^{(2n-1)}(\Gamma_1-1)(\Gamma_2-1)}, \end{aligned} (n = 1, 2, \ldots, +\infty) \tag{19}$$

It can be easily checked that the traction-free requirement that $Re\ \{f_i(\zeta)\}$, ($i = 1-3$) on the straight boundary $\delta = 0$ is still satisfied for the above obtained analytic functions $f_i(\zeta)$, ($i = 1-3$). It is observed that the derived analytic functions $f_i(\zeta)$, ($i = 1-3$) are expressed in infinite series forms.

Here we are particularly interested in the SIFs at the two crack tips, which are the most important parameters in fracture mechanics [6]. The closed-form expressions of the SIFs at the two crack tips can be exactly extracted from the obtained analytic functions $f_1(\zeta)$ and $f_3(\zeta)$ as follows

$$\begin{aligned} K_{\mathrm{III}}^{\mathrm{R}} &= \lim_{z\to a}\sqrt{2\pi|z-a|}\sigma_{zy} = \sigma_{zy}^{\infty}\sqrt{\tfrac{\pi(a^2-1)}{2a}}\tfrac{(2-\Gamma_1)\left[1+a^{-1}(\Gamma_2-1)\right]}{1-R(\Gamma_1-1)(\Gamma_2-1)}, \\ K_{\mathrm{III}}^{\mathrm{L}} &= \lim_{z\to a^{-1}}\sqrt{2\pi|z-a^{-1}|}\sigma_{zy} = \sigma_{zy}^{\infty}\sqrt{\tfrac{\pi(a^2-1)}{2a}}\tfrac{(2-\Gamma_2)[1+aR(\Gamma_1-1)]}{1-R(\Gamma_1-1)(\Gamma_2-1)}, \end{aligned} \tag{20}$$

where the superscripts R and L indicate the right and left crack tips, respectively. The reason why we can obtain closed-form expressions of the SIFs even though we can only derive series form solutions to the analytic functions $f_i(\zeta)$, ($i = 1-3$) is that in the ζ-plane the two crack tips are at $\zeta = 0$ and $\zeta = \infty$, consequently only A_1 and B_1, which are determined exactly in Eq. (19), are needed to evaluate the SIFs.

In the following we will illustrate the above results through several special cases:

(i) When $\mu_1 = \mu_2 = \mu_3$ ($\Gamma_1 = \Gamma_2 = 1$), then Eq. (20) reduces to

$$K_{\mathrm{III}}^{\mathrm{R}} = K_{\mathrm{III}}^{\mathrm{L}} = \sigma_{zy}^{\infty}\sqrt{\frac{\pi(a^2-1)}{2a}}, \tag{21}$$

which are just the well known results for a Griffith crack of total length $a - a^{-1}$ in a homogeneous material.

(ii) When $\mu_1 = \mu_2$ ($\Gamma_1 = 1$), then Eq. (20) reduces to

$$\begin{aligned} K_{\mathrm{III}}^{\mathrm{R}} &= \sigma_{zy}^{\infty}\sqrt{\tfrac{\pi(a^2-1)}{2a}}\left[1 + a^{-1}(\Gamma_2 - 1)\right], \\ K_{\mathrm{III}}^{\mathrm{L}} &= \sigma_{zy}^{\infty}\sqrt{\tfrac{\pi(a^2-1)}{2a}}(2-\Gamma_2), \end{aligned} \tag{22}$$

which are the results for a Griffith crack penetrating a single left circular inhomogeneity [4].

(iii) When $\mu_3 = \mu_2$ ($\Gamma_2 = 1$), then Eq. (20) reduces to

$$\begin{aligned} K_{\mathrm{III}}^{\mathrm{R}} &= \sigma_{zy}^{\infty}\sqrt{\tfrac{\pi(a^2-1)}{2a}}(2-\Gamma_1), \\ K_{\mathrm{III}}^{\mathrm{L}} &= \sigma_{zy}^{\infty}\sqrt{\tfrac{\pi(a^2-1)}{2a}}[1 + aR(\Gamma_1 - 1)], \end{aligned} \tag{23}$$

which are also the results for a Griffith crack penetrating a single right circular inhomogeneity [4].

(iv) When $\mu_1 = \mu_3$ ($\Gamma_1 = \Gamma_2 = \Gamma$), then Eq. (18) reduces to

$$\begin{aligned} K_{\mathrm{III}}^{\mathrm{R}} &= \sigma_{zy}^{\infty}\sqrt{\tfrac{\pi(a^2-1)}{2a}}\tfrac{(2-\Gamma)\left[1+a^{-1}(\Gamma-1)\right]}{1-R(\Gamma-1)^2}, \\ K_{\mathrm{III}}^{\mathrm{L}} &= \sigma_{zy}^{\infty}\sqrt{\tfrac{\pi(a^2-1)}{2a}}\tfrac{(2-\Gamma)[1+aR(\Gamma-1)]}{1-R(\Gamma-1)^2}. \end{aligned} \tag{24}$$

Particularly when the two inhomogeneities have the same unit radius we have $a^2R = 1$. Consequently it follows from Eq. (24) that $\sigma_{zy}^{\infty}(2-\Gamma)\sqrt{\frac{\pi(a^2-1)}{2a}} < K_{\mathrm{III}}^{\mathrm{R}} = K_{\mathrm{III}}^{\mathrm{L}} < \sigma_{zy}^{\infty}\sqrt{\frac{\pi(a^2-1)}{2a}}$ if the two inhomogeneities are softer than the matrix ($\Gamma > 1$); conversely $\sigma_{zy}^{\infty}(2-\Gamma)\sqrt{\frac{\pi(a^2-1)}{2a}} > K_{\mathrm{III}}^{\mathrm{R}} = K_{\mathrm{III}}^{\mathrm{L}} > \sigma_{zy}^{\infty}\sqrt{\frac{\pi(a^2-1)}{2a}}$ if the two inhomogeneities are stiffer than the matrix ($\Gamma < 1$). The above indicates that two *identical* inhomogeneities will reduce the shield or anti-shielding effect on a Griffith crack tip lodged in an isolated inhomogeneity.

(v) The SIFs at the two crack tips are exactly the same (i.e., $K_{\mathrm{III}}^{\mathrm{R}} = K_{\mathrm{III}}^{\mathrm{L}}$) when the following condition is met

$$\frac{\mu_2}{\mu_3} = \frac{a(1+aR)}{a+1}\frac{\mu_2}{\mu_1} + \frac{1-a^2R}{a+1}, \tag{25}$$

which indicates that $K_{\mathrm{III}}^{\mathrm{R}} \neq K_{\mathrm{III}}^{\mathrm{L}}$ if one inhomogeneity is stiffer while another one is softer than the matrix.

4. A screw dislocation in the matrix

Here we consider a screw dislocation with Burgers vector b located at $z = z_0$ in the matrix. By adopting a method identical to that used previously for the case of remote uniform loading, we can also obtain series form solutions to the three analytic functions $f_i(\zeta)$, $(i = 1-3)$. Here we will not list their specific lengthy expressions. The closed-form expressions of the SIFs at the two crack tips due to the screw dislocation at $z = z_0$ in the matrix can be finally determined as follows

$$\begin{aligned} K_{\mathrm{III}}^{\mathrm{R}} &= b\mu_2\sqrt{\frac{a}{2\pi(a^2-1)}}\frac{(2-\Gamma_1)\left\{1+a^{-1}(1-\Gamma_2)-\cos\frac{\theta_1-\theta_2}{2}\left[\sqrt{\frac{r_2}{r_1}}+a^{-1}(1-\Gamma_2)\sqrt{\frac{r_1}{r_2}}\right]\right\}}{1-R(\Gamma_1-1)(\Gamma_2-1)}, \\ K_{\mathrm{III}}^{\mathrm{L}} &= -b\mu_2\sqrt{\frac{a}{2\pi(a^2-1)}}\frac{(2-\Gamma_2)\left\{1+aR(1-\Gamma_1)-\cos\frac{\theta_1-\theta_2}{2}\left[\sqrt{\frac{r_1}{r_2}}+aR(1-\Gamma_1)\sqrt{\frac{r_2}{r_1}}\right]\right\}}{1-R(\Gamma_1-1)(\Gamma_2-1)}, \end{aligned} \tag{26}$$

where $z_0 - a = r_1\exp(\mathrm{i}\theta_1)$ and $z_0 - 1/a = r_2\exp(\mathrm{i}\theta_2)$. In the above expressions we have adopted the two-center bipolar coordinates with centers at $(1/a, 0)$ and $(a, 0)$ as illustrated in Fig. 1. It is observed that the above expressions are surprisingly simple once the two-center bipolar coordinates are adopted. Next we discuss several special cases to illustrate the obtained solutions.

(i) When $\mu_1 = \mu_2 = \mu_3$ ($\Gamma_1 = \Gamma_2 = 1$), then Eq. (26) reduces to

$$\begin{aligned} K_{\mathrm{III}}^{\mathrm{R}} &= b\mu_2\sqrt{\frac{a}{2\pi(a^2-1)}}\left(1-\sqrt{\frac{r_2}{r_1}}\cos\frac{\theta_1-\theta_2}{2}\right), \\ K_{\mathrm{III}}^{\mathrm{L}} &= -b\mu_2\sqrt{\frac{a}{2\pi(a^2-1)}}\left(1-\sqrt{\frac{r_1}{r_2}}\cos\frac{\theta_1-\theta_2}{2}\right), \end{aligned} \tag{27}$$

which are the results for a screw dislocation interacting with a finite Griffith crack in a homogeneous material.

(ii) When $\mu_1 = \mu_2$ ($\Gamma_1 = 1$), then Eq. (26) reduces to

$$\begin{aligned} K_{\mathrm{III}}^{\mathrm{R}} &= b\mu_2\sqrt{\frac{a}{2\pi(a^2-1)}}\left\{1+a^{-1}(1-\Gamma_2)-\cos\frac{\theta_1-\theta_2}{2}\left[\sqrt{\frac{r_2}{r_1}}+a^{-1}(1-\Gamma_2)\sqrt{\frac{r_1}{r_2}}\right]\right\}, \\ K_{\mathrm{III}}^{\mathrm{L}} &= -b\mu_2\sqrt{\frac{a}{2\pi(a^2-1)}}(2-\Gamma_2)\left(1-\sqrt{\frac{r_1}{r_2}}\cos\frac{\theta_1-\theta_2}{2}\right), \end{aligned} \tag{28}$$

which can be proved to be equivalent to our recent results for a finite Griffith crack penetrating a single left circular inhomogeneity with the dislocation located in the matrix [4].

(iii) When the screw dislocation is just located on the straight line which is vertical to the crack surface and which intersects the crack at the midpoint of the crack, we have $r_1 = r_2$ and $\theta_1 = \pi - \theta_2$. Consequently Eq. (26) reduces to

$$\begin{aligned} K_{\mathrm{III}}^{\mathrm{R}} &= b\mu_2\sqrt{\frac{a}{2\pi(a^2-1)}}\frac{2\cos^2\theta_2(2-\Gamma_1)\left[1+a^{-1}(1-\Gamma_2)\right]}{1-R(\Gamma_1-1)(\Gamma_2-1)} > 0, \\ K_{\mathrm{III}}^{\mathrm{L}} &= -b\mu_2\sqrt{\frac{a}{2\pi(a^2-1)}}\frac{2\cos^2\theta_2(2-\Gamma_2)[1+aR(1-\Gamma_1)]}{1-R(\Gamma_1-1)(\Gamma_2-1)} < 0. \end{aligned} \tag{29}$$

(iv) When the screw dislocation is just on the left circular interface, we have $r_1 = ar_2$. Consequently Eq. (26) reduces to

$$\begin{aligned} K_{\mathrm{III}}^{\mathrm{R}} &= b\mu_2\sqrt{\frac{a}{2\pi(a^2-1)}}\frac{(2-\Gamma_1)\left\{1+a^{-1}(1-\Gamma_2)-a^{-1/2}(2-\Gamma_2)\cos\frac{\theta_1-\theta_2}{2}\right\}}{1-R(\Gamma_1-1)(\Gamma_2-1)}, \\ K_{\mathrm{III}}^{\mathrm{L}} &= -b\mu_2\sqrt{\frac{a}{2\pi(a^2-1)}}\frac{(2-\Gamma_2)\left\{1+aR(1-\Gamma_1)-a^{1/2}[1+R(1-\Gamma_1)]\cos\frac{\theta_1-\theta_2}{2}\right\}}{1-R(\Gamma_1-1)(\Gamma_2-1)}. \end{aligned} \tag{30}$$

(v) When the screw dislocation is just on the right circular interface, we have $r_1 = aRr_2$. Consequently Eq. (26) reduces to

$$\begin{aligned} K_{\mathrm{III}}^{\mathrm{R}} &= b\mu_2\sqrt{\frac{a}{2\pi(a^2-1)}}\frac{(2-\Gamma_1)\left\{1+a^{-1}(1-\Gamma_2)-\frac{1+R(1-\Gamma_2)}{\sqrt{aR}}\cos\frac{\theta_1-\theta_2}{2}\right\}}{1-R(\Gamma_1-1)(\Gamma_2-1)}, \\ K_{\mathrm{III}}^{\mathrm{L}} &= -b\mu_2\sqrt{\frac{a}{2\pi(a^2-1)}}\frac{(2-\Gamma_2)\left\{1+aR(1-\Gamma_1)-\sqrt{aR}(2-\Gamma_1)\cos\frac{\theta_1-\theta_2}{2}\right\}}{1-R(\Gamma_1-1)(\Gamma_2-1)}. \end{aligned} \tag{31}$$

5. A screw dislocation within the right inhomogeneity

In this case the closed-form expressions of the SIFs at the two crack tips due to a screw dislocation with Burgers vector b at $z = z_0$ in the right inhomogeneity can be finally determined as follows

$$\begin{aligned}
K_{\mathrm{III}}^{\mathrm{R}} &= b\mu_2\sqrt{\frac{a}{2\pi(a^2-1)}}\frac{2-\Gamma_1}{\Gamma_1}\left\{\frac{\Gamma_1\left[1+a^{-1}(1-\Gamma_2)\right]}{1-R(\Gamma_1-1)(\Gamma_2-1)}+\cos\frac{\theta_1-\theta_2}{2}\left[\sqrt{\frac{r_1}{r_2}}\frac{a^{-1}(\Gamma_2-1)-(aR)^{-1}(\Gamma_1-1)}{1-R(\Gamma_1-1)(\Gamma_2-1)}-\sqrt{\frac{r_2}{r_1}}\right]\right\},\\
K_{\mathrm{III}}^{\mathrm{L}} &= -b\mu_2\sqrt{\frac{a}{2\pi(a^2-1)}}\frac{(2-\Gamma_2)\left[1+aR(1-\Gamma_1)+(\Gamma_1-2)\sqrt{\frac{r_1}{r_2}}\cos\frac{\theta_1-\theta_2}{2}\right]}{1-R(\Gamma_1-1)(\Gamma_2-1)}.
\end{aligned}\tag{32}$$

When $\mu_1 = \mu_2$ ($\Gamma_1 = 1$), Eqs. (26) and (32) are exactly the same. When the screw dislocation is just on the right interface by letting $r_1 = aRr_2$, Eq. (32) will just reduce to Eq. (31).

When $\mu_3 = \mu_2$ ($\Gamma_2 = 1$), then Eq. (32) reduces to

$$\begin{aligned}
K_{\mathrm{III}}^{\mathrm{R}} &= b\mu_2\sqrt{\frac{a}{2\pi(a^2-1)}}\frac{2-\Gamma_1}{\Gamma_1}\left\{\Gamma_1-\cos\frac{\theta_1-\theta_2}{2}\left[\sqrt{\frac{r_2}{r_1}}+(aR)^{-1}(\Gamma_1-1)\sqrt{\frac{r_1}{r_2}}\right]\right\},\\
K_{\mathrm{III}}^{\mathrm{L}} &= -b\mu_2\sqrt{\frac{a}{2\pi(a^2-1)}}\left[1+aR(1-\Gamma_1)+(\Gamma_1-2)\sqrt{\frac{r_1}{r_2}}\cos\frac{\theta_1-\theta_2}{2}\right],
\end{aligned}\tag{33}$$

which are the results for a finite crack penetrating a single right circular inhomogeneity with the dislocation within the right inhomogeneity.

When the screw dislocation is just at the center of the right inhomogeneity, we have $\sqrt{r_1} = aR\sqrt{r_2}$. In this case it follows from Eq. (32) that

$$\begin{aligned}
K_{\mathrm{III}}^{\mathrm{R}} &= -b\mu_2\sqrt{\frac{(1-aR)^2}{2\pi aR^2(a^2-1)}}\frac{(2-\Gamma_1)[1+R(\Gamma_2-1)]}{\Gamma_1[1-R(\Gamma_1-1)(\Gamma_2-1)]}<0,\\
K_{\mathrm{III}}^{\mathrm{L}} &= -b\mu_2\sqrt{\frac{a(1-aR)^2}{2\pi(a^2-1)}}\frac{2-\Gamma_2}{1-R(\Gamma_1-1)(\Gamma_2-1)}<0,
\end{aligned}\tag{34}$$

which indicate that the screw dislocation at the center of the right inhomogeneity always has a shielding effect ($K_{\mathrm{III}}^{\mathrm{R}}, K_{\mathrm{III}}^{\mathrm{L}} < 0$) on the two crack tips.

6. A screw dislocation within the left inhomogeneity

In this case the closed-form expressions of the SIFs at the two crack tips due to a screw dislocation of Burgers vector b at $z = z_0$ in the left inhomogeneity can be finally determined as follows

$$\begin{aligned}
K_{\mathrm{III}}^{\mathrm{R}} &= b\mu_2\sqrt{\frac{a}{2\pi(a^2-1)}}\frac{(2-\Gamma_1)\left[1+a^{-1}(1-\Gamma_2)+(\Gamma_2-2)\sqrt{\frac{r_2}{r_1}}\cos\frac{\theta_1-\theta_2}{2}\right]}{1-R(\Gamma_1-1)(\Gamma_2-1)},\\
K_{\mathrm{III}}^{\mathrm{L}} &= -b\mu_2\sqrt{\frac{a}{2\pi(a^2-1)}}\frac{2-\Gamma_2}{\Gamma_2}\left\{\frac{\Gamma_2[1+aR(1-\Gamma_1)]}{1-R(\Gamma_1-1)(\Gamma_2-1)}+\cos\frac{\theta_1-\theta_2}{2}\left[\sqrt{\frac{r_2}{r_1}}\frac{aR(\Gamma_1-1)+a(1-\Gamma_2)}{1-R(\Gamma_1-1)(\Gamma_2-1)}-\sqrt{\frac{r_1}{r_2}}\right]\right\}.
\end{aligned}\tag{35}$$

When $\mu_3 = \mu_2$ ($\Gamma_2 = 1$), Eqs. (26) and (35) are exactly the same. When the screw dislocation is just on the left interface by letting $r_1 = ar_2$, Eq. (35) will just reduce to Eq. (30).

When the screw dislocation is just at the center of the left inhomogeneity, we have $\sqrt{r_1} = a\sqrt{r_2}$. In this case it follows from Eq. (32) that

$$\begin{aligned}
K_{\mathrm{III}}^{\mathrm{R}} &= b\mu_2\sqrt{\frac{a-1}{2\pi a(a+1)}}\frac{2-\Gamma_1}{1-R(\Gamma_1-1)(\Gamma_2-1)}>0,\\
K_{\mathrm{III}}^{\mathrm{L}} &= b\mu_2\sqrt{\frac{a(a-1)}{2\pi(a+1)}}\frac{(2-\Gamma_2)[1+R(\Gamma_1-1)]}{\Gamma_2[1-R(\Gamma_1-1)(\Gamma_2-1)]}>0,
\end{aligned}\tag{36}$$

which indicates that a screw dislocation at the center of the left inhomogeneity always exerts an anti-shielding effect ($K_{\mathrm{III}}^{\mathrm{R}}, K_{\mathrm{III}}^{\mathrm{L}} > 0$) on the two crack tips.

7. A Zener-Stroh crack

In the following we consider the case in which the finite crack $[1/a\ a]$ is a Zener-Stroh crack [10,11]. The sum of the Burgers vectors inside the Zener-Stroh crack is

$$\int_{1/a}^{a}\left[w_{,x}(x,0^-)-w_{,x}(x,0^+)\right]\mathrm{d}x = b.\tag{37}$$

In this case the closed-form expressions of the SIFs at the two tips of the Zener-Stroh crack with a total Burgers vector b can be finally determined as follows

$$K_{\mathrm{III}}^{\mathrm{R}}=b\mu_2\sqrt{\frac{a}{2\pi(a^2-1)}}\frac{(2-\Gamma_1)\left[1+a^{-1}(1-\Gamma_2)\right]}{1-R(\Gamma_1-1)(\Gamma_2-1)}>0,$$
$$K_{\mathrm{III}}^{\mathrm{L}}=-b\mu_2\sqrt{\frac{a}{2\pi(a^2-1)}}\frac{(2-\Gamma_2)[1+aR(1-\Gamma_1)]}{1-R(\Gamma_1-1)(\Gamma_2-1)}<0. \tag{38}$$

The above results can also be obtained from either one of Eqs. (26), (32) and (35) by letting a screw dislocation approach the (Griffith) crack surfaces ($\theta_1-\theta_2=\pm\pi$) so that $\cos\frac{\theta_1-\theta_2}{2}=0$.

It is of interest to discuss the following special cases:

(i) When $\mu_1=\mu_2=\mu_3$ ($\Gamma_1=\Gamma_2=1$), then Eq. (38) reduces to

$$K_{\mathrm{III}}^{\mathrm{R}}=-K_{\mathrm{III}}^{\mathrm{L}}=b\mu_2\sqrt{\frac{a}{2\pi(a^2-1)}}, \tag{39}$$

which are the results for a Zener-Stroh crack in a homogeneous material [4,12].

(ii) When $\mu_1=\mu_2$ ($\Gamma_1=1$), then Eq. (38) reduces to

$$K_{\mathrm{III}}^{\mathrm{R}}=b\mu_2\sqrt{\frac{a}{2\pi(a^2-1)}}[1+a^{-1}(1-\Gamma_2)],$$
$$K_{\mathrm{III}}^{\mathrm{L}}=-b\mu_2\sqrt{\frac{a}{2\pi(a^2-1)}}(2-\Gamma_2), \tag{40}$$

which are the results for a Zener-Stroh crack penetrating a single left inhomogeneity [4].

(iii) When $\mu_3=\mu_2$ ($\Gamma_2=1$), then Eq. (38) reduces to

$$K_{\mathrm{III}}^{\mathrm{R}}=b\mu_2\sqrt{\frac{a}{2\pi(a^2-1)}}(2-\Gamma_1),$$
$$K_{\mathrm{III}}^{\mathrm{L}}=-b\mu_2\sqrt{\frac{a}{2\pi(a^2-1)}}[1+aR(1-\Gamma_1)], \tag{41}$$

which are also the results for a Zener-Stroh crack penetrating a single right inhomogeneity [4].

(iv) When $\mu_1=\mu_3$ ($\Gamma_1=\Gamma_2=\Gamma$), then Eq. (38) reduces to

$$K_{\mathrm{III}}^{\mathrm{R}}=b\mu_2\sqrt{\frac{a}{2\pi(a^2-1)}}\frac{(2-\Gamma)\left[1+a^{-1}(1-\Gamma)\right]}{1-R(\Gamma-1)^2},$$
$$K_{\mathrm{III}}^{\mathrm{L}}=-b\mu_2\sqrt{\frac{a}{2\pi(a^2-1)}}\frac{(2-\Gamma)[1+aR(1-\Gamma)]}{1-R(\Gamma-1)^2}. \tag{42}$$

Particularly when the two inhomogeneities have the same unit radius we have $a^2R=1$. Consequently it follows from Eq. (42) that $K_{\mathrm{III}}^{\mathrm{R}}=-K_{\mathrm{III}}^{\mathrm{L}}<b\mu_2(2-\Gamma)\sqrt{\frac{a}{2\pi(a^2-1)}}<b\mu_2\sqrt{\frac{a}{2\pi(a^2-1)}}$ if the two inhomogeneities are softer than the matrix ($\Gamma>1$); conversely $K_{\mathrm{III}}^{\mathrm{R}}=-K_{\mathrm{III}}^{\mathrm{L}}>b\mu_2(2-\Gamma)\sqrt{\frac{a}{2\pi(a^2-1)}}>b\mu_2\sqrt{\frac{a}{2\pi(a^2-1)}}$ if the two inhomogeneities are stiffer than the matrix ($\Gamma<1$). The above indicates that two identical inhomogeneities will enhance the shield or anti-shielding effect on a Zener-Stroh crack tip lodged in an isolated inhomogeneity.

(v) $K_{\mathrm{III}}^{\mathrm{R}}=-K_{\mathrm{III}}^{\mathrm{L}}$ when the following condition is satisfied

$$\frac{\mu_2}{\mu_3}=\frac{a(1-aR)}{a-1}\frac{\mu_2}{\mu_1}-\frac{1-a^2R}{a-1}, \tag{43}$$

which indicates that $K_{\mathrm{III}}^{\mathrm{R}}\neq-K_{\mathrm{III}}^{\mathrm{L}}$ if one inhomogeneity is stiffer while another one is softer than the matrix.

8. Related problems

Instead of a finite crack [$1/a$ a], we now consider the related problem of a circular hole partially merged in two circular inhomogeneities, as shown in Fig. 4. The radius of the circular hole is $(a-1/a)/2$ and its center is at $z=(a+1/a)/2$. Apparently the circular hole intersects the two circular inhomogeneities at a common vertex angle $\pi/2$. This geometry is an extension of the 2D snowman type of an object studied by Palaniappan [6]. The three-phase composite is only subjected to remote uniform shearing σ_{zy}^{∞}. Now we consider the following conformal mapping function

$$z=\frac{\zeta-a}{a\zeta-1}. \tag{44}$$

The mapped ζ-plane is shown in Fig. 5 ($\zeta=\delta+\mathrm{i}\eta$). The traction-free surface of the circular hole is mapped onto the straight boundary $\delta=0$ in the ζ-plane. In the ζ-plane we can derive series form solutions to this problem. The specific solution procedures are suppressed here. Particularly we are interested in the stress concentration factors (SCFs) $\sigma_{zy}/\sigma_{zy}^{\infty}$ at the two points $z=a$ and $z=1/a$. The closed-form expressions of the SCFs can be finally derived as

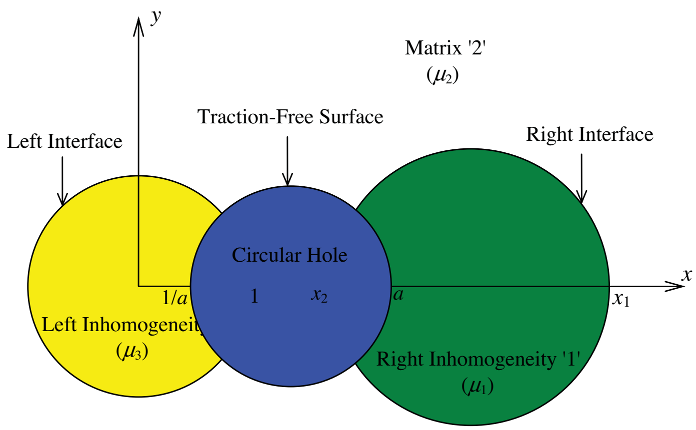

Fig. 4. A circular hole partially merged in two circular inhomogeneities in the original z-plane.

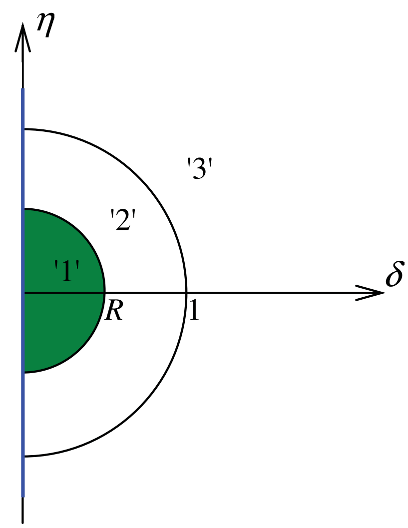

Fig. 5. The mapped ζ-plane for a circular hole partially merged in two circular inhomogeneities.

$$\frac{\sigma_{zy}}{\sigma_{zy}^{\infty}} = \frac{2(2-\Gamma_1)[1+a^{-2}(\Gamma_2-1)]}{1-R^2(\Gamma_1-1)(\Gamma_2-1)}, \quad \text{at } z=a, \tag{45}$$

$$\frac{\sigma_{zy}}{\sigma_{zy}^{\infty}} = \frac{2(2-\Gamma_2)[1+a^2R^2(\Gamma_1-1)]}{1-R^2(\Gamma_1-1)(\Gamma_2-1)}, \quad \text{at } z=1/a. \tag{46}$$

As well known the SCF is 2 for a circular hole in a homogeneous material under remote uniform antiplane shearing. Eqs. (45) and (46) give us extremely simple formulae to calculate the SCFs for a circular hole partially merged in two circular inhomogeneities. Not restricted to the above, we can further consider a more general situation: a *hole* formed by two circular arcs with their two common tips at $z = a$ and $z = 1/a$ partially merged in two circular inhomogeneities.

9. Conclusions

The main part of this research is devoted to the study of a Mode-III finite crack partially penetrating two circular inhomogeneities under the following loading conditions: (i) remote uniform anti-plane shearing; (ii) a straight screw dislocation at any position of the three-phase system; (iii) a Zener-Stroh crack. Closed-form expressions of the SIFs were derived in Eq. (20) due to remote uniform shearing; Eq. (26) due to a screw dislocation in the matrix; Eq. (32) due to a screw dislocation within the right inhomogeneity; Eq. (35) due to a screw dislocation within the left inhomogeneity; Eq. (38) due to a Zener-Stroh crack. It is observed that the expressions of SIFs due to a screw dislocation become strikingly simple once the two-center bipolar coordinates with the centers at the two crack tips are adopted.

As a byproduct of this investigation, we also addressed a circular hole partially merged in two circular inhomogeneities. Closed-form expressions of the SCFs were obtained. In fact our method can be extended to address the more general situation of a hole formed by two circular arcs with their two common tips at $z = a$ and $z = 1/a$ partially merged in two circular inhomogeneities.

Acknowledgements

One reviewer's comments and suggestions were highly appreciated. The first author (X.W.) was supported by Innovation Program of Shanghai Municipal Education Commission (No. 12ZZ058), and research grants at ECUST. The second author (E.P.) was supported in part by AFRL/ARL.

References

[1] F. Erdogan, G.D. Gupta, The inclusion problem with a crack crossing the boundary, Int. J. Fract. 11 (1975) 13–27.
[2] P.S. Steif, A semi-infinite crack partially penetrating a circular inclusion, J. Appl. Mech. 54 (1987) 87–93.
[3] Y.P. Wang, R. Ballarini, A long crack penetrating a circular inhomogeneity, Meccanica 38 (2003) 579–593.
[4] X. Wang, E. Pan, W.J. Feng, Closed-form solutions for a mode III radial matrix crack penetrating a circular inhomogeneity, Appl. Math. Model. 32 (2008) 2925–2935.
[5] E. Honein, T. Honein, G. Herrmann, On two circular inclusions in harmonic problems, Q. Appl. Math. 50 (1992) 479–499.
[6] A.T. Zehnder, Lecture Notes on Fracture Mechanics, Cornell University, 2007.
[7] D. Palaniappan, Classical image treatment of a geometry composed of a circular conductor partially merged in a dielectric cylinder and related problems in electrostatics, J. Phys.: Math. & Gen. 38 (2005) 6253–6269.
[8] W.J. Cao, Conformal Mapping Theory and Its Application, Shanghai Science and Technology Publisher, 1988.
[9] N.I. Muskhelishvili, Some Basic Problems of the Mathematical Theory of Elasticity, P. Noordhoff Ltd, Netherlands, 1963.
[10] C. Zener, The micro-mechanism of fracture, Fracturing of Metals, American Society for Metals, Cleveland, 1948. 3–31.
[11] A.N. Stroh, The formation of cracks as a result of plastic flow, I, Proc. Roy. Soc. London A 223 (1954) 404–414.
[12] Z.M. Xiao, B.J. Chen, Electro-elastic stress analysis for a Zener-Stroh crack interacting with a coated inclusion in a piezoelectric solid, Acta Mech. 171 (2004) 29–40.